

A New Dynamic Powder Consolidation Technique Using Shock Waves

Jheison Lopes dos Santos^{a,b}, Rubens Lincoln Santana Blazutti Marçal^a, Sérgio Neves Monteiro^a,
Luis Henrique Leme Louro^a*

^a*Instituto de Engenharia Militar (IME), Department of Materials Science, Praça General Tibúrcio, 80, Praia Vermelha, CEP 22290-270, Urca, Rio de Janeiro, RJ, Brazil.*

^b*Universidade Estácio de Sá (UNESA), Department of Production Engineering, Rua Lemos, 21, Santa Cruz, CEP 23510-160, Rio de Janeiro, RJ, Brazil.*

Received: December 12, 2016; Revised: June 6, 2017; Accepted: June 20, 2017

Techniques for shock consolidation of powders have been developed for different purposes, including the synthesis of diamond from carbon powder. In this work, a new device configuration for dynamic consolidation is proposed. It consists of three coaxial tubes, with a conical cover made of explosive at the top of the device. The inner tube contains the powder to be compacted. The second is accelerated towards the first in order to promote its collapse. The third confines the explosive. A conical cap at the top of the device triggers the explosive. For a preliminary evaluation, two types of explosives, TNT and Composition B, were used. Preliminary analytical results by the impedance matching method indicate that maximum pressures of 35.44 GPa and 48.16 GPa could be achieved using TNT and Composition B, respectively. Maximum temperatures around 1,600 K and 2,500 K for TNT and Composition B, respectively, are expected. These pressure and temperature values are adequate for transforming graphite into diamond. Preliminary Rietveld refinement indicated that nanodiamond is a fraction of approximately 54% of the detonation resulting powder.

Keywords: *consolidation, detonation, synthesis, dynamic compression.*

1. Introduction

Shock wave consolidation and synthesis of materials has been investigated since 1960's¹⁻¹⁴ for many purposes, including the synthesis of diamonds from carbon powder¹⁵⁻²⁷. This process is associated with the use of explosives. Upon detonation, a high-pressure shock wave is generated that moves into the main explosive, initiating the reaction. Figure 1 presents a detonation wave scheme. The front of this wave moves toward the unreacted material with a speed D . The interface between the unreacted explosive and the front of the detonation wave has a high peak pressure, called the von Neumann peak, which is narrow and quickly attenuated. Between the unreacted explosive and detonation of the explosive products, there is a region named chemical reaction zone. It performs the transformation of solid explosive into gaseous detonation products.

The interface between the chemical reaction region and the detonation products is where the synthesis is completed. This is called the Chapman-Jouguet point (C-J), used to characterize the explosive, i.e., its pressure (P_{CJ}) and particle velocity (U_{pCJ})²⁸. The wave of relaxation, known as Taylor wave, propagates into the product immediately behind the detonation wave²⁸. The phenomenon of dynamic deformation at high rates due to detonation shock wave is governed by conservation relationships that were derived from Rankine-Hugoniot²⁸⁻³¹. The following equations represent, respectively, the conservations of mass, momentum and energy.

$$\rho_0 \cdot D = \rho \cdot (D - U_p). \quad (1)$$

$$(P - P_0) = \rho_0 \cdot D \cdot U_p. \quad (2)$$

$$(E - E_0) = U_p^2 / 2 + Q. \quad (3)$$

where ρ_0 is the initial specific mass; ρ , the final specific mass; D , the detonation wave velocity; U_p , the particle velocity; P , the final pressure; P_0 , the initial pressure; E , the final energy; E_0 , the initial energy; V , the final volume; V_0 , the initial volume, and Q is the chemical energy per mass unit.

The conservation equations, (1), (2) e (3), involve 5 variables. So, one additional equation is required to relate them. Then, it is also used an experimentally obtained equation of state shown in Eq. 4.

$$U_s = C_0 + S \cdot U_p. \quad (4)$$

where S is an empirical parameter and C_0 a characteristic sound wave velocity.

Some previous methods use substantial amounts of explosives, in the order of up to hundreds of pounds. Besides that, there are methods that combine distinct types of explosives which can generate difficulties, such as good interaction of different explosives, and interface effects as well. With the present method, only about 2 kg of a single type of explosive was used in each detonation for similar

* e-mail: lopesjheison@gmail.com

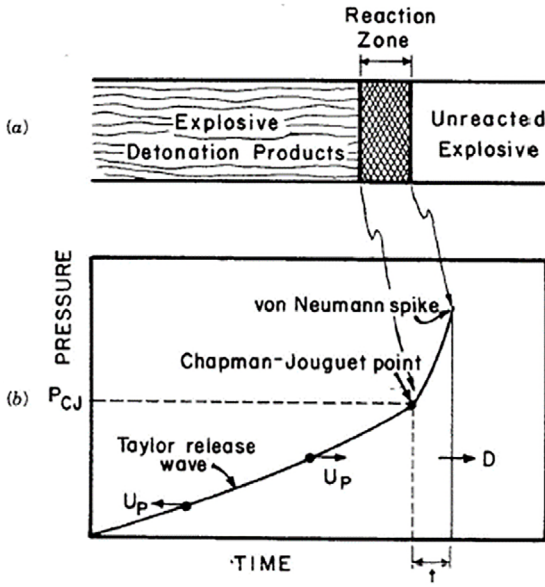


Figure 1. (a) The structure of a detonation shock wave, and (b) the pressure as a function of time (adapted from Meyers²⁸).

purpose. This contributes to minimizing the cost of confection of the device, including the amount of explosive, making it possible to increase the number of tests to be performed.

2. Materials and Methods

As aforementioned, this new configuration is proposed to transform a carbon precursor powder into diamond. Then, as such precursor, carbon black (Quimesp, 98% purity) was used. Upon transformation, a fast quench is necessary to maintain the diamond structure. Thus, copper powder (Viner Brasil Tecnologia, 99,6% purity) was chosen as quenching medium, given its known high thermal conductivity. The carbon black and copper powder were mixed, with a weight ratio of 10/90, respectively, to ensure greater homogeneity and satisfactory cooling to achieve the desired transformation.

The new design for dynamic consolidation is a round configuration consisting of three concentric cylinders in the form of tubes. Meyers and Wang⁶ were the first to use this technique with the purpose of promote powder synthesis by shock wave. Subsequently, Ferreira⁹ improved it. From the device successfully used by Meyers⁶, an adaptation has been made, shown schematically in Figure 2. This new design requires less explosive and successfully yields comparatively more diamonds than previous ones^{6,9}. This novel technique here proposed is the startup through a single explosive in conical shape at the top of the double tube device. The intermediate cylinder, called flyer tube (diameter of 1.5 in.), is made of the same inner stainless steel tube (diameter of 3/4 in.). The flyer tube is accelerated inward by the shock wave produced by the detonation of TNT (trinitrotoluene) and Composition B (hexolite, 60wt% RDX and 40wt% TNT) that collapse the inner tube containing the powder to

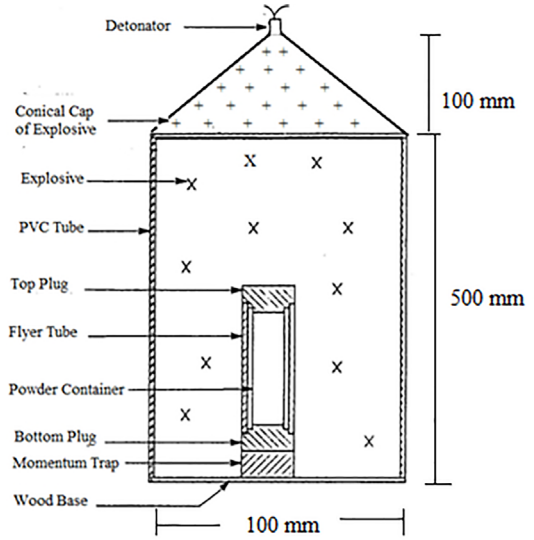


Figure 2. Schematic representation of the proposed device (adapted from Meyers²⁸), with the conical cap made of explosive.

be synthesized. These tubes are 304 stainless steel and 300 mm high. High pressure and elevated temperature achieved by the shock wave are favorable conditions for carbon transformation into the diamond structure^{17,18,23,26,27,28}. Between the steel tubes, there is an empty space that is required for accelerating the flyer tube against the inner tube containing the powder. The external tube, made of PVC, with 500 mm of height and 100 mm of diameter, confines the explosive. The explosives were cast and poured into the device. Then, its solidification was made with the device immersed in flowing water at room temperature.

It is expected that the detonation wave of the conical explosive cap (also with 100 mm diameter), initiated by the detonator, reaches the cap/explosive interface as a plane wave, given the distance to be traveled and the speed of the detonation wave^{6,28}.

The calculation of the pressure generated by the shock wave at the moment of the impact was estimated using the shock impedance matching method²⁸. This is given by the intersection of the direct Hugoniot from the target material with the inverted Hugoniot from the impacting material. The relation between the impact velocity of the flyer tube and the ratio of the masses of the flyer tube and of the charge (M/C) follows the Gurney's equation³¹ for cylindrical configuration, presented by Eq. 5.

$$V_p = \sqrt{2E} \sqrt{\frac{3}{\left(\frac{5M}{C} + 2\left(\frac{M}{C}\right)^2 \left(\frac{R+r_0}{r_0}\right) + \left(\frac{2r_0}{R+r_0}\right)\right)}} \quad (5)$$

A sequence of dynamic relationships permitted the evaluation of the pressure at the C-J point¹⁸.

The P x U_p direct Hugoniot of the materials may be calculated by Eq. 6.

$$P = \rho_0 \cdot (C_0 + S \cdot U_p) \cdot U_p \quad (6)$$

and its P x Up inverted Hugoniot, presented as follow.

$$P = \rho_0 \cdot [C_0 + S \cdot (V - U_p)] \cdot (V - U_p). \quad (7)$$

were V is the impact velocity. The P x Up inverted Hugoniot of the explosive is given by.

$$P = \frac{1}{2} \cdot \rho_0 \cdot (V - U_p)^2 (\gamma + 1) + Q \rho_0 \cdot (\gamma - 1). \quad (8)$$

and the pressure at the Chapman-Jouguet point (P_{CJ}) can be calculated by.

$$P_{CJ} = \rho_0 \cdot D^2 / (\gamma + 1). \quad (9)$$

where γ is the polytropic gas constant.

3. Results and Discussion

The first results were achieved considering the TNT explosive. All parameters involved were taken from Meyers²⁸. In order to obtain the pressure values in the flying tube P_{FT} and its respective particle velocity (U_p)_{FT} as well as the pressure in the copper powder, the values of the intersections of the Hugoniot curves of the materials involved were used, as seen in Figure 3.

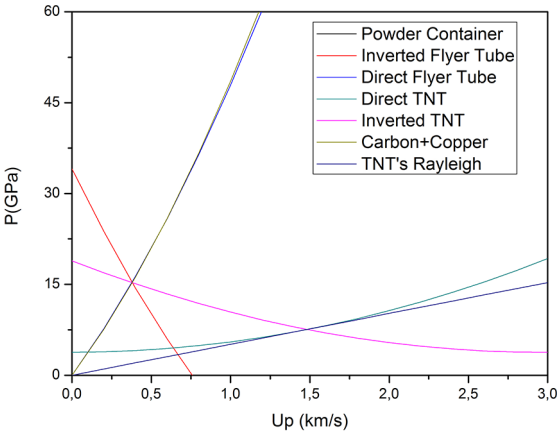


Figure 3. Hugoniot curves obtained by the detonation of TNT explosive.

Observing the graph, the point that intercepts the direct Hugoniot of the flyer tube with the inverted Hugoniot of the explosive provides P_{FT} \cong 36.50 GPa and (U_p)_{FT} \cong 801.47 m/s. One can also observe that the impact velocity of the flyer tube is about 1,602.94 m/s, which, in accord with the Gurney equation³¹. The dimensions of the device, provides an M/C ratio around 0.885.

The direct Hugoniot of the container of the powder to be compacted (copper with carbon) is hidden by the direct Hugoniot of the flyer tube because both are made of the same material. It is also seen in Figure 3 that the pressure

on the mixture powder, due the interaction with the stainless steel tube, was about 36.62 GPa, with particle velocity of 799.23 m/s.

Figure 4 illustrates the direct and inverted Hugoniots of the materials involved in the detonation of the Composition B explosive.

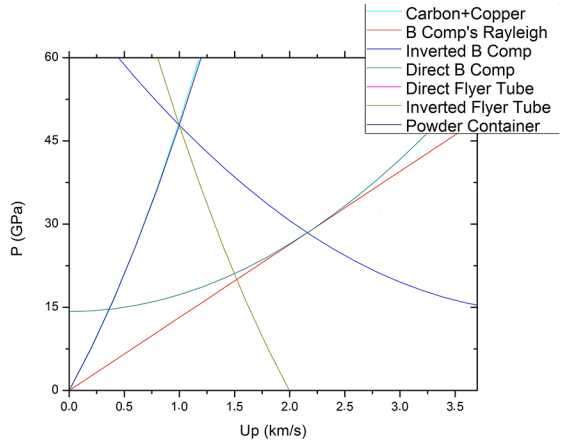


Figure 4. Hugoniot curves obtained by the detonation of Composition B explosive.

The intersection point of the direct Hugoniot of the flyer tube with the Composition B inverted Hugoniot gives P_{FT} \cong 47.85 GPa and (U_p)_{FT} \cong 999.52 m/s. The impact velocity of the flyer tube is about 1,999.04 m/s, providing an M/C ratio about 0.718. Besides that, one can observe that the pressure generated on the mixture of copper and carbon black was about 48.16 GPa, with particle velocity close to 994.46 m/s.

In order to estimate the temperature reached by the detonation, the method described by Meyers²⁸ to the temperature rise associated with shock waves was adopted. The standard solution is of the form shown in Eq. 10.

$$T = T_0 \exp\left[\left(\frac{\gamma_0}{V_0}\right)(V_0 - V)\right] + \frac{(V_0 - V)}{2Cv} P + \frac{\exp\left[\left(-\frac{\gamma_0}{V_0}\right)V\right]}{2Cv} \int_{V_0}^V P \exp\left[\left(\frac{\gamma_0}{V_0}\right)V\right] \left[2 - \left(\frac{\gamma_0}{V_0}\right) - (V_0 - V)\right] dV. \quad (10)$$

According to the values displayed on literature²⁸, a temperature of the order of 1,600 K is estimated for the TNT detonation, and about 2,500 K for the detonation of the Composition B explosive.

Such values of pressure and temperature, even for the TNT and Composition B explosives, achieved the diamond region on the carbon phase diagram presented in Figure 5.

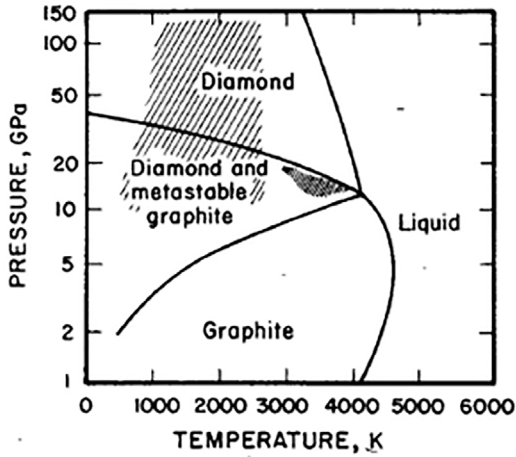


Figure 5. Pressure-temperature phase diagram of carbon (adapted from Meyers²⁸).

Rietveld refinement of the products obtained from the TNT explosive detonation was performed. It indicated that a considerable amount of detonation diamonds (more than 50%), with crystallite size about 29 nm, and GOF of 1.418, was achieved as can be seen in Figure 6. Moreover, experimental evidence of transformed diamond nanoparticles is shown in Figure 7.

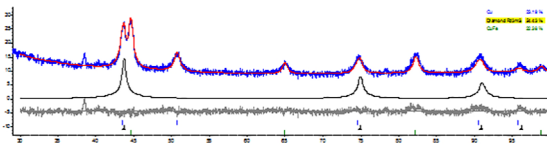


Figure 6. Rietveld refinement of the products obtained from the TNT explosive detonation.

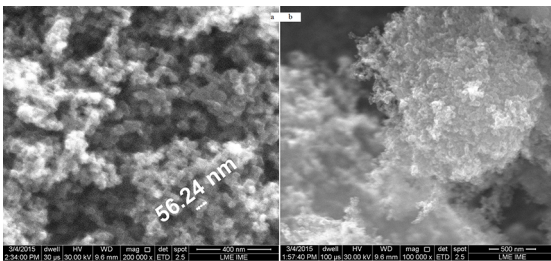


Figure 7. Micrographs of the nanodiamonds obtained by the detonation, at (a) 200,000X and (b) 100,000X.

Preliminary Raman spectroscopy analyses of the detonation product confirmed the presence of diamonds.

4. Conclusions

A different configuration for dynamic compaction of powder is suggested. It consists of a common double tube

configuration, with a conical single explosive cap initiation. The pressure, impact velocity and temperature values to be reached with the detonation of explosives were estimated. The shock wave generated by detonation TNT (trinitrotoluene) indicated a pressure around 35.44 GPa and a temperature of approximately 1,600 K, while the Composition B detonation provided a pressure of 48.16 GPa and a temperature of about 2,500 K. By the M/C ratio, it can be seen that the necessary quantity of explosives is relatively small (~2 kg), reducing the cost of the process. The preliminary experimental results of SEM, Rietveld refinement and Raman spectroscopy, confirmed the presence of transformed nanodiamonds, with estimated crystallite size of about 29 nm.

5. References

1. DeCarli PS, Jamieson JC. Formation of Diamond by Explosive Shock. *Science*. 1961;133(3467):1821-1822.
2. DeCarli PS, inventor. *Method of Making Diamond*. United States patent US 3238019. 1966 Mar 1.
3. Kestenback HJ, Meyers MA. The effect of grain size on the shock-loading response of 304-type stainless steel. *Metallurgical Transactions A*. 1976;7(12):1943-1950.
4. DeCarli JS, Meyers MA. Design of Uniaxial Strain Shock Recovery Experiments. In: Meyers MA, Murr LE, eds. *Shock Waves and High-Strain-Rate Phenomena in Metals – Concepts and Applications*. New York: Plenum; 1981. p. 341-373.
5. Graham RA, Sawaoka A, eds. *High Pressure Explosive Processing of Ceramics*. Basel: Trans Tech. Publications; 1987.
6. Meyers MA, Wang SL. An improved method for shock consolidation of powders. *Acta Metallurgica*. 1988;36(4):925-936.
7. Titov VM, Anisichkin VF, Mal'kov IY. Synthesis of ultradispersed diamond in detonation waves. *Combustion, Explosion and Shock Waves*. 1989;25(3):372-379.
8. Fritz JN. *A Simple Plane-Wave Explosive Lens*. Los Alamos: Los Alamos National Laboratory; 1990.
9. Ferreira A, Meyers MA, Thadhani NN, Chang SN, Kough JR. Dynamic compaction of titanium aluminides by explosively generated shock waves: Experimental and materials systems. *Metallurgical Transactions A*. 1991;22(3):685-695.
10. Huang L, Han WZ, An Q, Goddard WA III, Luo SN. Shock-induced consolidation and spallation of Cu nanopowders. *Journal of Applied Physics*. 2012;111(1):013508.
11. Mashhadi HA, Bataev I, Sadeghi BM, Hokamoto K. Mechanochemical synthesis and shock wave consolidation of TiN(Al) nanostructure solid solution. *Materials Chemistry and Physics*. 2014;145(3):366-375.
12. Yin A, Chen P, Xu C, Gao X, Zhou Q, Zhao Y, et al. Shock-wave synthesis of multilayer graphene and nitrogen-doped graphene materials from carbonate. *Carbon*. 2015;94:928-935.
13. Bai JS, Wang X, Pei XY, Wang Y, Yu YY, Shen Q, et al. Improved Impactor Design for Eliminating Spallation in High-Impedance Flyers During Hypervelocity Launch. *Experimental Mechanics*. 2016;56(9):1661-1664.

14. Mitrofanov VV, Titov VM. On mixing of the products of detonation of composite explosives in the chemical reaction region. *Combustion, Explosion, and Shock Waves*. 2016;52(5):587-592.
15. Deribas AA, Simonov PA, Filimonenko VN, Shtertser AA. Long-pulse explosive compacting of diamond powder. In: Staudhammer KP, Murr LE, Meyers MA, eds. *Fundamental Issues and Applications of Shock-Wave and High-Strain Rate Phenomena*. Oxford: Elsevier Science; 2001. p. 331-336.
16. Kozyrev NV, Sakovich GV, Sou ST. Investigation of Diamond Synthesis from a Mixture of an Explosive with a Carbon Additive Using a Tracer Technique. *Combustion, Explosion, and Shock Waves*. 2005;41(5):589-590.
17. Shenderova O, Gruen D, eds. *Ultrananocrystalline Diamond: Synthesis, Properties and Applications*. Oxford: William Andrew; 2006.
18. Kozyrev NV, Larionov BV, Sakovich GV. Influence of HMX Particle Size on the Synthesis of Nanodiamonds in Detonation Waves. *Combustion, Explosion, and Shock Waves*. 2008;44(2):193-197.
19. Kurdyumov AV, Britun VF, Yarosh VV, Solonin YM, Borimchuk, NI, Zelyavskii VB, et al. Shock-wave synthesis of diamond nanofibers and their structure. *Journal of Superhard Materials*. 2011;33(1):13-18.
20. Shenderova OA, Koscheev A, Zapiro N, Petrov I, Skryabin Y, Detkov P, et al. Surface Chemistry and Properties of Ozone-Purified Detonation Nanodiamonds. *Journal of Physical Chemistry C*. 2011;115(20):9827-9837.
21. Shenderova OA, Vlasov II, Turner S, Tendeloo GV, Orlinskii SB, Shiryayev AA, et al. Nitrogen Control in Nanodiamond Produced by Detonation Shock-Wave-Assisted Synthesis. *Journal of Physical Chemistry C*. 2011;115(29):14014-14024.
22. Niu KY, Zheng HM, Li ZQ, Yang J, Sun J, Du XW. Laser Dispersion of Detonation Nanodiamonds. *Angewandte Chemie*. 2011;50(18):4099-4102.
23. Mochalin VN, Shenderova OA, Ho D, Gogotsi Y. The properties and applications of nanodiamonds. *Nature Nanotechnology*. 2012;7:11-23.
24. Kaur R, Badea I. Nanodiamonds as novel nanomaterials for biomedical applications: drug delivery and imaging systems. *International Journal of Nanomedicine*. 2013;8:203-220.
25. Presti C, Alauzun JG, Laurencin D, Mutin PH. Surface Functionalization of Detonation Nanodiamonds by Phosphonic Dichloride Derivatives. *Langmuir*. 2014;30(30):9239-9245.
26. Dolgoborodov A, Brazhnikov M, Makhov M, Gubin S, Maklashova I. Detonation performance of high-dense BTF charges. *Journal of Physics: Conference Series*. 2014;500(Pt 5):052010.
27. Kirmani AR, Peng W, Mahfouz R, Amassian A, Losovyj Y, Idriss H, et al. On the relation between chemical composition and optical properties of detonation nanodiamonds. *Carbon*. 2015;94:79-84.
28. Meyers MA. *Dynamic Behavior of Materials*. Hoboken: John Wiley & Sons; 1994.
29. Rankine WJM. On the Thermodynamic Theory of Waves of Finite Longitudinal Disturbance. *Philosophical Transactions of the Royal Society of London*. 1870;160:277-286.
30. Hugoniot PH. Mémoire sur la propagation du mouvement dans les corps et plus spécialement dans les gaz parfaits. 2^e Partie. *Journal de l'École Polytechnique*. 1889;58:1-125.
31. Gurney RK. *The Initial Velocities of Fragments from Bombs, Shells, and Grenades*. Aberdeen Proving Ground: BRL Report 405 Ballistic Research Laboratory; 1943.